P- ISSN 1991-8941 E-ISSN 2706-6703
2025,(19), (01):137 – 149

Journal of University of Anbar for Pure Science (JUAPS)

Open Access

Synthesis, Characterization, and Thermal Study of Nickel Complexes with Schiff base and Mixed Ligands and their Analytical Application

Wesal Sadiq Ahmed*, Sattar Rajb Majeed

Department of Chemistry, College of Science, University of Anbar, Ramadi, Iraq:
wis22s3001@uoanbar.edu.iq, sat70tar@uoanbar.edu.iq

ARTICLE INFO

Received: 30 / 05 /2024
Accepted: 07/ 08 /2024
Available online: 19/ 06 /2025

DOI: 10.37652/juaps.2024.150382.1266

Keywords:
Nickel, Schiff base, Mixed ligands, Thermal studies, Mole ratio.

ABSTRACT

Nickel(II) complexes were synthesized using the Schiff base ligands (E)-4-((2-hydroxybenzylidene)amino)-1,5-dimethyl-2-phenyl-1,2-dihydro-3H-pyrazol-3-one, ($C_{18}H_{17}N_3O_2$) as the primary ligand in combination of oxalic acid, malonic acid, and sodium pyrophosphate as secondary ligands. The reactions were carried out in a 1:) mole ratio, resulting in the formation of [Ni($C_{18}H_{17}N_3O_2$)(Cl_2)], [Ni($C_{18}H_{17}N_3O_2$)(ox)], [Ni($C_{18}H_{17}N_3O_2$)(ma)], and [Ni($C_{18}H_{17}N_3O_2$)(pyph)]. The synthesized complexes were characterized through elemental microanalysis, atomic absorption spectroscopy, mass spectroscopy, thermal gravimetric analysis, FT-IR spectroscopy, UV spectroscopy, molar conductivity measurements, and melting point determination. The complexes were found to adopt a square-planer geometry, and maximum absorbance was observed at 429 nm under optimal reaction conditions. Results suggested that the synthesized complexes are non-electrolyte. The Schiff base ligands (E)-4-((2-hydroxybenzylidene)amino)-1,5-dimethyl-2-phenyl-1,2-dihydro-3H-pyrazol-3-one, oxalic acid, and malonic acid, and sodium pyrophosphate behaved as bidentate ligands, coordinating with Ni(II) ions. Based on the cumulative evidence obtained through these techniques, a square-planar geometry was proposed for all the complexes. Furthermore, (E)-4-((2-hydroxybenzylidene)amino)-1,5-dimethyl-2-phenyl-1,2-dihydro-3H-pyrazol-3-one was found to be a viable chromogenic sensor for the spectral analysis of nickel ions. The formation of highly colored complexes with Ni(II) produced distinct absorption peaks, enabling quantitative analysis of nickel at the microgram level through calibration curves.

Introduction

Since the discovery of $CoCl_3 \cdot 6NH_3$ in 1789, coordinated chemical compounds have attracted considerable interest. The field of chemistry has considerably advanced in the latter part of the 20th century, driven by rapid developments in the synthesis of complex coordination molecules and its contribution to understanding their structures.[1] Schiff bases have been demonstrated to be effective ligands because of their facile production and extensive chelating capabilities for several metal ions. Additionally, they have the ability to readily form stable complexes with most transition metals.

Schiff bases are organic compounds with the general formula RC = NR, which are formed by the condensation of an amine with a ketone or aldehyde.

Schiff bases are highly adaptable ligands capable of acting as donor molecules with bidentate, tridentate, tetradentate, or hexadentate coordination modes.[2] Schiff base compounds have extensive applications as chelating ligands in coordination chemistry. Additionally, they have practical applications in various fields, such as catalysis and medicine, where they are utilized as antibiotics, antiallergic drugs, and anticancer agents.[3] Heterocyclic compounds derived from 4-aminoantipyrine are of particular interest because of their natural abundance and broad range of pharmacological effects. The coordination

*Corresponding author at : Department of Chemistry, College of Science, University of Anbar, Ramadi, Iraq
ORCID:https:// https://orcid.org/0009-0006-0475-5410,
Tel: +964 7821462276
Email: wis22s3001@uoanbar.edu.iq

characteristics of 4-aminoantipyrine can be modified by combining its main amino group with the carbonyl group of an aldehyde or ketone. This modification results in the formation of novel ligands with potentially enhanced properties.[4] The ortho position adjacent to a azomethine group contains a hydroxyl group, which is generated by the interaction of amine and aldehyde groups.[5] The majority of Schiff bases exhibit a remarkable ability to coordinate with metal ions, forming stable complex compounds with main group elements, transition metal, lanthanide, and actinide elements. This interaction considerably enhances the properties of resulting complexes. The stability of these complexes is attributed to the bonding of the azomethine (N = CH) lone pair of electrons in their structure.[6] Coordination compounds are often employed in the fields of metallurgy, industrial catalysts, and analytical reagents, and several coordination chemicals are utilized in electroplating and textile dyeing.[7] Schiff base transition metal complexes are intriguing structures in coordination chemistry because of their exceptional pharmacological potential, which are determined by the quantity of donor atoms and the oxidation state of metal ions. Among various transition metals, complexes formed with the 3d series are durable metal–organic molecules that have considerably advanced the field of organometallic chemistry owing to their remarkable effectiveness and relatively low cost.[8] Nickel, a vital trace element for humans, animals, microbes, and plants, is present in several enzymes, where it plays a critical role in key metabolic events.[9] Considerable interest has been directed toward the study of nickel and palladium complexes with multidentate Schiff base ligands because of their crucial role in bioinorganic chemistry and redox enzyme systems. These complexes have the potential as structural models for the active sites of biological systems or as catalysts.[10]

Materials and Methods

Materials

The chemicals were of analytical grade and used without further purification. These chemicals include nickel chloride (Sigma Aldrich), oxalic acid, malonic acid, tetrasodium pyrophosphate (Fluka), dimethyl sulfoxide, dimethyl formamide, acetone, and ethanol (Sigma Aldrich).

Instrument

Melting points were determined using a Stuart SMP20 melting point system. Electronic spectra were recorded in dimethylformamide (DMF) with a double-beam Shimadzu UV–Vis spectrophotometer. Infrared spectroscopy was conducted using a Bruker Shimadzu instrument. Conductivity measurements were carried out at 25 °C with a HANNAEC214 conductivity meter. Elemental analysis was performed using a EuroVector EA 3000 elemental analyzer (version 3.0). Mass spectra were obtained using a Shimadzu Qp-2010 Plus gas chromatograph. Thermal gravimetric analysis was conducted using a Shimadzu THA-05 DSC-60 DTG-60H instrument. pH was measured using pH meter. Atomic absorption measurements were performed using a Shimadzu atomic absorption and flame emission spectrophotometer (AA680).

Methodology

Schiff base ligand ((E)-4-((2-hydroxybenzylidene)amino)-1,5-dimethyl-2-phenyl-1,2-dihydro-3H-pyrazol-3-one)($C_{18}H_{17}N_3O_2$)

Aminoantipyrine (0.2 g, 0.01 mole) dissolved in absolute ethanol (5 mL) was mixed with salicylaldehyde (0.9 mL; 0.01 mole) containing glacial acetic acid (2 drops). Then, the mixture was refluxed at 80 °C for 3 h under continuous stirring. Then, the solution was allowed to cool at room temperature, and the precipitate was filtered, washed with ethanol and diethyl ether, and dried. The yield was 80%.[11]

Preparation of nickel complexes

Synthesis of the [Ni($C_{18}H_{17}N_3O_2$)(CI_2)] complex

A complex was prepared by dissolving 0.129 g (0.001 mole) of nickel chloride salt ($NiCl_2$) in 15 mL of absolute ethanol, and concentrated hydrochloric acid (HCl) was added dropwise to ensure complete dissolution under stirring and heating. Subsequently, the primary ligand solution (0.307 g, 0.001 mol) dissolved in 15 mL of ethanol was added dropwise, and the pH was adjusted to 6. The mixture was then heated at 80 °C for 3 h under continuous stirring. After cooling to room

temperature, the complex was filtered and washed with diethyl ether. The yield was 60%.

Synthesis of the [Ni($C_{18}H_{17}N_3O_2$)(ma)] complex

$NiCl_2$ (0.129 g; equivalent to 0.001 moles) were dissolved in 15 mL of ethanol. Concentrated hydrochloric acid was added dropwise to ensure complete dissolution under stirring and heating. Then, a solution containing 0.307 g (0.001 moles) of the primary ligand $C_{18}H_{17}N_3O_2$ was added to the mixture, followed by a solution containing 0.104 g (0.001 moles) of the secondary ligand malonic acid in 10 mL of ethanol. The mixture was stirred, and the pH was adjusted to 7. The entire mixture was heated for 3 h under constant agitation at 80 °C. Subsequently, the solution was allowed to cool to ambient temperature, and the solid material was separated by filtration. The solid was then washed with ethanol and diethyl ether and dried. The yield was 40%

Synthesis of [Ni($C_{18}H_{17}N_3O_2$)ox] complex

$NiCl_2$ (0.129 g; 0.001 moles) was dissolved in 15 mL of ethanol. Concentrated HCl was added dropwise to ensure complete dissolution under continuous stirring and heating. Subsequently, 0.307 g (0.001 moles) of a primary ligand solution dissolved in 15 mL of ethanol was gradually added to the mixture under stirring. Finally, a secondary ligand solution containing oxalic acid (0.09 g; 0.001 moles) dissolved in 10 mL of ethanol was added. The pH of the mixture was adjusted to 7. The resulting mixture was heated for 3 h under constant stirring at a temperature of 80°C. Subsequently, the solution was allowed to cool to room temperature, and the resulting solid was separated by filtration. The solid was then washed with ethanol and diethyl ether and finally dried. The yield was 40%.

Synthesis of [Ni($C_{18}H_{17}N_3O_2$)pyph] complex

$NiCl_2$ (0.129 g; 0.001 moles) was dissolved in 15 mL of ethanol. Concentrated HCl was added dropwise to ensure complete dissolution under stirring and heating. Then, a solution of the primary ligand (0.307 g; 0.001 moles) dissolved in 15 mL of ethanol was added dropwise while stirring. Subsequently, a secondary ligand solution (pyrophosphate tetrasodium) weighing 0.444 g (0.001 moles) in 15 mL of ethanol was added to the mixture under stirring. The pH of the solution was adjusted to 7. The entire mixture was heated for 3 h under continuous stirring at 80 °C. Afterward, the solution was cooled to room temperature, and the resulting solid was separated by filtration. The solid was then washed with ethanol and diethyl ether and finally dried. The yield was 70%.

Results and Discussion

Four nickel complexes were prepared with a Schiff base ligand as a primary ligand and malonic acid, oxalic acid, and tetrasodium pyrophosphate as secondary ligands. The properties of the complexes and methods for their characterization are summarized in **Table (3-1)**.

Table (3-1) Physical properties of the prepared complexes

NO	Compound	Molecular weight (g/mol)	Color	Yield (%)	Melting point (°C)	Molar conductivity
1	$C_{18}H_{17}N_3O_2$	307	Bright yellow	80%	210	……
2	[Ni($C_{18}H_{17}N_3O_2$)(Cl_2)]	436	Light green	60%	250	17.4
3	[Ni($C_{18}H_{17}N_3O_2$)(ma)]	468	green	40%	>300	15
4	[Ni($C_{18}H_{17}N_3O_2$)(ox)]	454	green	40%	>300	13
5	[Ni($C_{18}H_{17}N_3O_2$)(pyph)]	585	Dark green	70%	>300	7

Table (3-2) Results of microanalysis of the elements

NO	compounds	%C	H%	N%	Ni%	Cl%	O%
1	$[Ni(C_{18}H_{17}N_3O_2)Cl_2]$	49.54 (48.97)	4.01 (2.94)	9.63 (10,83)	13.30 (13.43)	16.10 16.23	7.33 (7.32)
2	$[Ni(C_{18}H_{17}N_3O_2)(ma)]$	46.05 (45.69)	3.73 (4.22)	8.95 (9.94)	12.39 (12.54)	....	20.51 (21.51)
3	$[Ni(C_{18}H_{17}N_3O_2)(ox)]$	47.68 (46.88)	3.86 (3.08)	9.27 (10.35)	12.77 (12.93)	....	21.14 (22.24)
4	$[Ni(C_{18}H_{17}N_3O_2)(pyph)]$	36.92 (36.90)	1.98 (2.92)	7.17 (7.17)	9.91 (10.02)	....	24.61 (24.57)

Table (3-3) Solubility of the complexes

	complex	water	ethanol	acetone	DMF	DMSO
1	$(C_{18}H_{17}N_3O_2)$	_	+	+	+	+
2	$[Ni(C_{18}H_{17}N_3O_2)CI_2]$	_	÷	÷	+	+
3	$[Ni(C_{18}H_{17}N_3O_2)(ma)]$	_	÷	÷	+	+
4	$[Ni(C_{18}H_{17}N_3O_2)(ox)]$	_	÷	÷	+	+
5	$[Ni(C_{18}H_{17}N_3O_2)$ (Phyh)]	–	÷	÷	+	+

(+) = soluble, (_) = insoluble, and (÷) = sparingly soluble

UV–Vis spectra

The electronic spectra of the ligand and nickel complexes were recorded at 200–1000 nm using DMF solution and quartz cells. The ligand exhibits spectrum bands at 266 and 355 nm. The band at 266 nm is due to π → *π transitions in the benzene rings and amine groups, whereas the band at 355 nm is due n → *π transitions in the nonbonding electrons of nitrogen atoms. $[Ni(C_{18}H_{17}N_3O_2)Cl_2]$ exhibits a π → *π transition at 265 nm and a red shift from 355 nm to 380 nm. These results indicates the formation of the complex and the coordination between the imine group and the central metal ion.[12] In the $[Ni(C_{18}H_{17}N_3O_2)(ma)]$ complex, a peak appeared at 264 nm, which is attributed to the electronic transition π → *π. Another peak was observed at 355 nm, which corresponds to the electronic transition n → *π. Additionally, absorption bands at 542 and 986 nm are assigned to d-d transitions.[13] In the $[Ni(C_{18}H_{17}N_3O_2)(ox)]$ complex, an absorption peak appeared at 263 nm corresponds to the electron transition π → *π, whereas the peaks at 353 and 372 nm correspond to transition n → *π transitions. Additionally, a peak at 542 nm is assigned to a d-d transition.[3] In $[Ni(C_{18}H_{17}N_3O_2)(pyph)]$, an absorption peak at 256 nm corresponds to π → *π transition, a peak at 356 nm to a n → *π transition, a peak at 429 nm to a charge transfer. A d-d transition was observed at 542 nm.[10]

Table (3-4) Results of UV–Vis measurements of complexes

NO	Compound	Wave length (nm)	Wave number (cm^{-1})	Transition
1	$(C_{18}H_{17}N_3O_2)$	266 355	37593 28169	π → *π n → *π
2	$[Ni(C_{18}H_{17}N_3O_2)Cl_2]$	204 260 380	49019 38461 28089	n → *σ π → *π n → *π
3	$[Ni(C_{18}H_{17}N_3O_2)(ma)]$	264 355 542 986	37878 28169 18450 10141	π → *π n → *π d-d d-d
4	$[Ni(C_{18}H_{17}N_3O_2)(ox)]$	263 353 372 542	38022 28328 26881 18450	π → *π n → *π n → *π d-d
5	$[Ni(C_{18}H_{17}N_3O_2)(Pyph)]$	256 356 429 542	39062 28089 23310 18450	π → *π n → *π C.T d-d

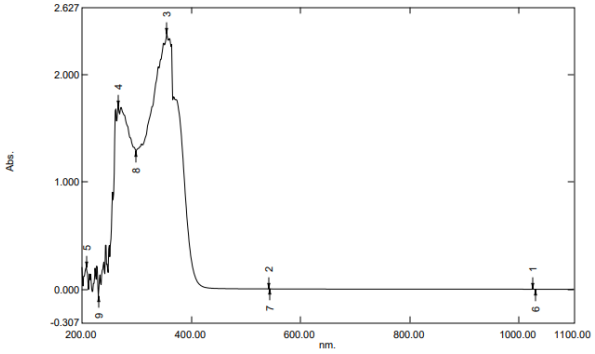

Figure (3-1) Electronic spectrum of the ligand $(C_{18}H_{17}N_3O_2)$

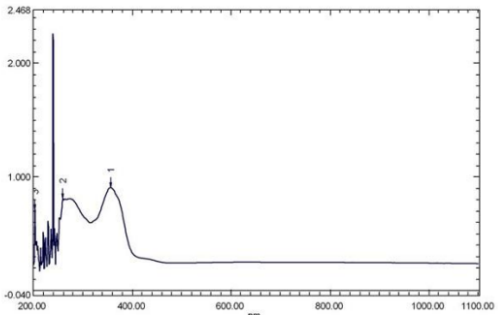

Figure (3-2) Electronic spectrum of the complex [Ni($C_{18}H_{17}N_3O_2$)(CI_2)]

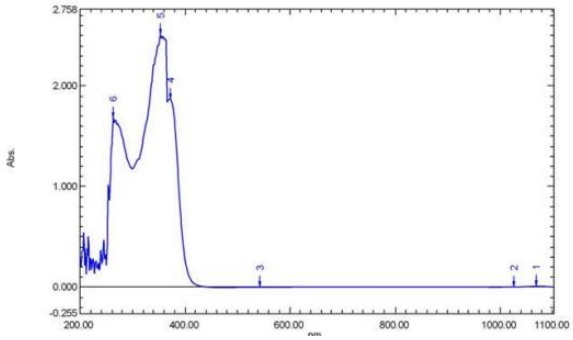

Figure (3-4) Electronic spectrum of complex [Ni($C_{18}H_{17}N_3O_2$)(ox)]

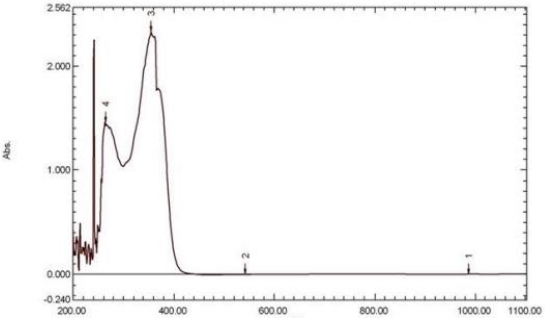

Figure (3-3) Electronic spectrum of the complex [Ni($C_{18}H_{17}N_3O_2$)(ma)]

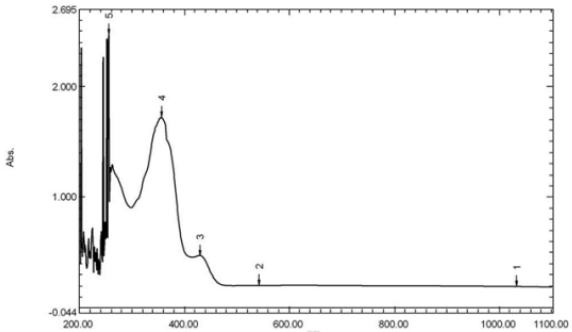

Figure (3-5) Electronic spectrum of the complex [Ni($C_{18}H_{17}N_3O_2$)(Phyh)]

Infrared spectral data

In the infrared spectra, all complexes and ligands were measured and characterized in a range of 400–4000 cm^{-1}. A comparison between the absorption spectra of the free ligand and complexes was conducted to confirm the coordination of the ligand with the central metal ion. The observed shifts in the absorption wavelengths toward higher or lower frequencies serve as evidence of the ligand's involvement in complex formation.[14] In the four prepared complexes, the displacement of the imine group from 1589 cm^{-1} to 1519 cm^{-1}.[15] The OH group from 3672 cm^{-1} to 3435 cm^{-1} indicates their involvement in complex formation. The C=O group exhibited a slight shift of approximately 30 cm^{-1}, from 1619 cm^{-1} to 1587 cm^{-1}, because it did not participate in the coordination and formation of the complexes. We observed new bonds at 500–520, which correspond to the bonds between N and the central metal Ni. The new band at 416–460 nm was attributed to the bond between O and Ni.[2]

Table (3-5) FT-IR spectrum of primary ligand and complexes

NO	C=O	C=N	C=C	OH	CH3	CH2	N-Ni	N-O
L	1619	1589	1486	3672	2934	3100	.....	.....
[Ni($C_{18}H_{17}N_3O_2$)(CI_2)]	1610	1544	1489	3452	2885	3109	503	423
[Ni($C_{18}H_{17}N_3O_2$)(ma)]	1651	1593	1489	3435	2926	3055	516	430
[Ni($C_{18}H_{17}N_3O_2$)(ox)]	1651	1489	1413	3404	2937	3061	519	428
[Ni($C_{18}H_{17}N_3O_2$)(Phyh)]	1610	1546	1485	3444	2927	3105	522	449

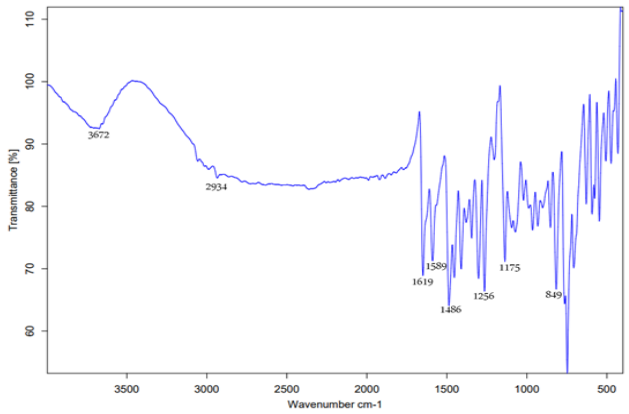

Figure (3-6) FT-IR spectrum of Schiff base ligand

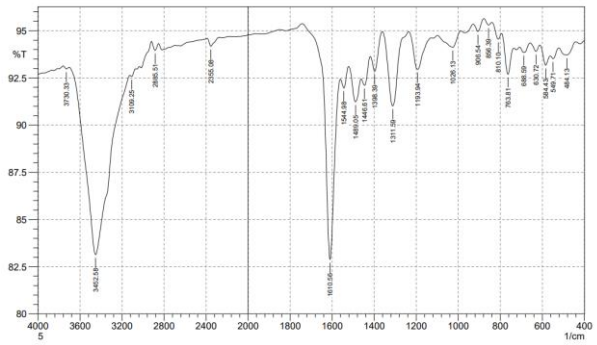

Figure (3-7) FT-IR spectrum of complex [Ni($C_{18}H_{17}N_3O_2$)CI_2]

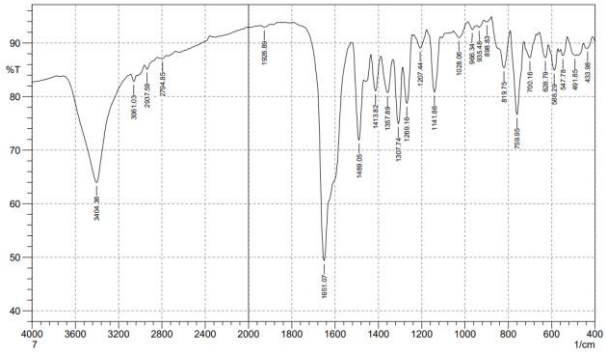

Figure (3-9) FT-IR spectrum of complex [Ni($C_{18}H_{17}N_3O_2$)(ox)]

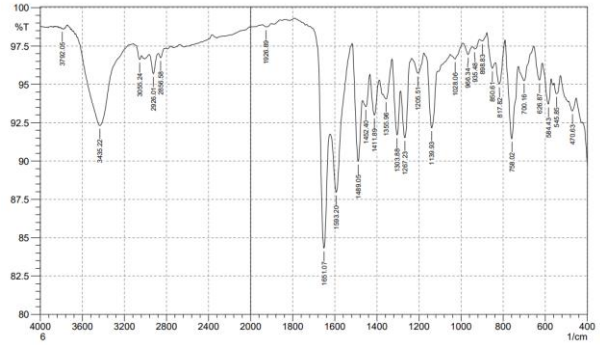

Figure (3-8) FT-IR spectrum of complex [Ni($C_{18}H_{17}N_3O_2$)(ma)]

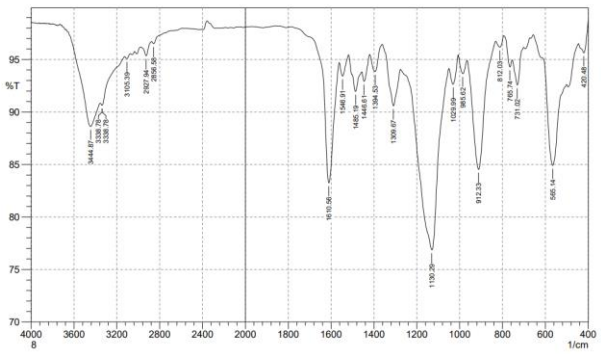

Figure (3-10) FT-IR spectrum of complex [Ni($C_{18}H_{17}N_3O_2$)(Phyh)]

Mass spectra

The mass spectrum of [Ni ($C_{18}H_{17}N_3O_2$)Cl2] (M. wt = 436 g l mole) displayed a parent peak at mlz of 436, as shown in **Figure (3-11)**.

The mass spectrum of [Ni ($C_{18}H_{17}N_3O_2$)(ma)] (M. wt = 468 g l mole) displayed a parent peak at mlz of 469, as shown in **Figure (3-12)**.

The mass spectrum of [Ni ($C_{18}H_{17}N_3O_2$)(ox)] (M. wt = 454 g l mole) displayed a parent peak at mlz of 453, as shown in **Figure (3-13)**.

The mass spectrum of compound [Ni($C_{18}H_{17}N_3O_2$)(pyph)] (M. wt = 585 g l mole) displayed a parent peak at mlz of 585, as shown in **Figure (3-14)**

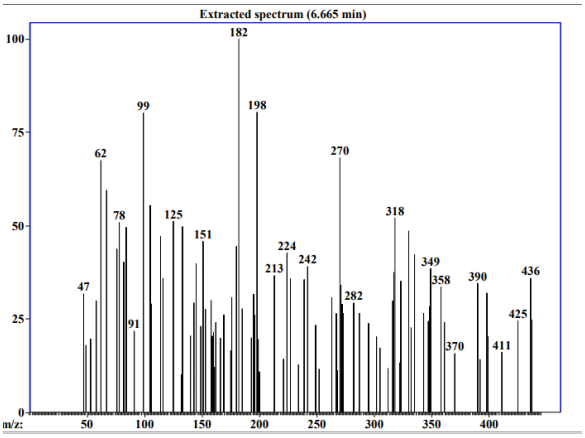

Figure (3-11) Mass spectrum of [Ni ($C_{18}H_{17}N_3O_2$)Cl_2]

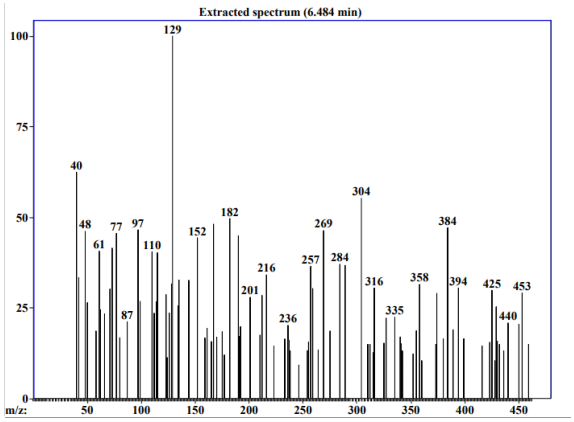

Figure (3-13) Mass spectrum of [Ni($C_{18}H_{17}N_3O_2$)(ox)]

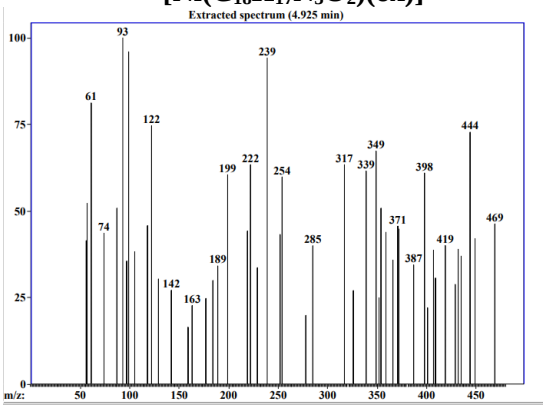

Figure (3-12) Mass spectrum of [Ni ($C_{18}H_{17}N_3O_2$)(ma)]

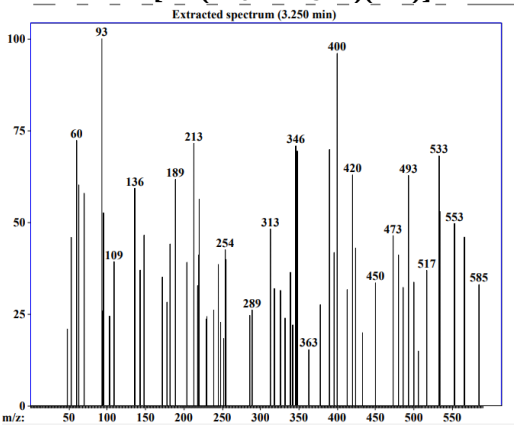

Figure (3-14) mass spectrum of complex [Ni ($C_{18}H_{17}N_3O_2$)(Pyph)]

Thermogravimetric analysis (TGA)

The thermal behavior of the reported complexes was characterized using a thermogravimetric analysis (TGA)-weight thermolysis curve. This technique measures mass change of a substance in a specific temperature range while subjecting it to a controlled heating program at a specific time. The resulting curve is referred to as the thermoweight curve. The curve provides information on thermal stability, reaction speed, model chemical composition, and output thermal stability. **Table (3-6)** presents results consistent with the proposed generic formula for complexes. The table also shows information for each stage of weight degradation, where Ti is The temperature at which the breakup begins for a given step, Tf is the temperature at which the breakup ends at that step, and Tmax is the maximum temperature of weight loss.

The TGA of the [($C_{18}H_{17}N_3O_2$)($NiCl_2$)] complex revealed a two-stage decomposition process, as shown in **Figure (3-17)**. **Figure (3-15)** shows the mechanism of the thermogravimetric decomposition of the complex, the critical temperature at which the maximum transformation of the compound occurs (maximum weight loss), and the practical and theoretical percentage lost from each indicator stage. The total mass loss is 74.666%, and the residual mass is 25.334%). These results align with theoretical values, which predict a total mass loss of 74.616% and remaining mass of 25.383%. The residual product is consistent with the formation of (NiO + 3C) according to the proposed mechanism.[16] The thermogravimetric decomposition of the [C21H19N3O6Ni] complex proceeded in two stages, as shown in the **Figure (3-18)**. **Figure (3-15)** displays outlines the thermal breakdown pathway of the complex, identifies the critical temperature corresponding to the maximum rate of mass loss, and compares the experimentally observed mass loss with the theoretically calculated values at each decomposition stage.[17] The TGA of [$C_{20}H_{17}N_{3O6}Ni$] revealed a total mass loss of 64.528% and remaining mass of 35.471%. The theoretically calculated mass loss is 63.515%, and the remaining mass is 36.484%. The residue is consistent with the formation (NiO + 8C) in accordance with the proposed mechanism. The two-stage decomposition process is illustrated in **Figure (3-19)**. **Figure (3-16)** presents the mechanism of the thermogravimetric decomposition of the complex, the critical temperature at which the maximum transformation of the compound occurs (maximum weight loss), and the practical and theoretical percentage loss at each stage. The total mass loss is 64.3417%, and the remaining mass is 35.6583%. The theoretically calculated mass loss is 65.0352%, and the remaining

mass is 34.9648%. The residue is (NiO + 7C) according to the proposed mechanism.[18] The [C18H17N3O9NiNa2P2] complex also decomposed in two stages, as shown in **Figure (3-20)**. **Figure 3-16** illustrates the thermogravimetric decomposition mechanism of the complex, the critical temperature at which the compound undergoes maximum transformation (maximum weight loss), and the practical and theoretical percentages of mass loss at each stage. The obtained mass loss is 62.2%, and the remaining mass is 37.8%. The theoretically calculated mass loss is 60.642%, and the remaining mass is 39.357%. The residue is NiO + 4C + 2Na + 2P according to the proposed mechanism.[19]

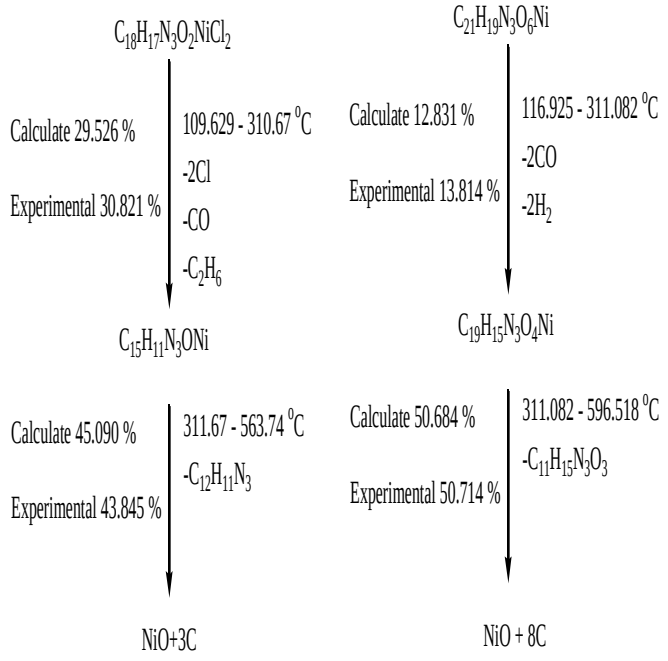

Figure (3-15) Scheme of thermal decomposition of the complex
[$C_{18}H_{17}N_3O_2PdCl_2$] and [$C_{21}H_{19}N_3O_6Pd$]

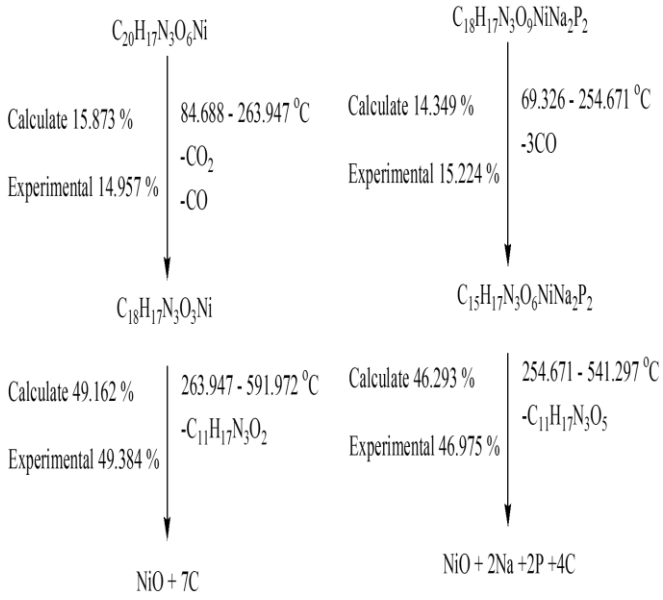

Figure (3-16) Scheme of thermal decomposition of the complex
[$C_{20}H_{17}N_3O_6Pd$] and [$C_{18}H_{17}N_3O_9PdNa_2P_2$]

Table (3-6) Thermal analysis of complexes

No	Thermo gravimetric range (°C)	DTG max (°C)	% Estimated (calculated)		Assignment
			Mass loss	Total	
1	109.629 – 310.67 310.67 – 563.74	215.94 429.84	30.821 (29.526) 43.845 (45.090)	74.666 (74.616)	CO + 2Cl + C_2H_6 $C_{12}H_{11}N_3$ Residue NiO + C_3
2	116.92 – 311.08 311.08 – 596.51	229.74 423.84	13.814 (12.831) 50.714 (50.684)	64.528 (63.515)	2CO + $2H_2$ $C_{11}H_{15}N_3O_3$ Residue NiO + C_8
3	84.688 – 263.947 263.947 – 591.972	169.84 408.99	14.9571 (15.873) 49.3846 (491622)	64.3417 (65.0352)	-CO + CO_2 - $C_{11}H_{17}N_3O_2$ Residue NiO + 7C

4	**69.326 – 254.671 254.671 –541.297**	**167.82 408.64**	**15.224 (14.349) 46.975 (46.293)**	**62.2 (60.642)**	**-3CO -$C_{11}H_{17}N_3O_5$ Residue NiO + 4C +2Na +2P**

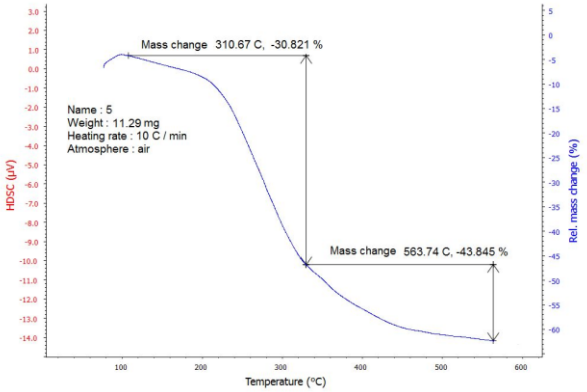

Figure (3-17) Thermal gravimetric of complex [$C_{18}H_{17}N_3O_2$ Ni Cl_2]

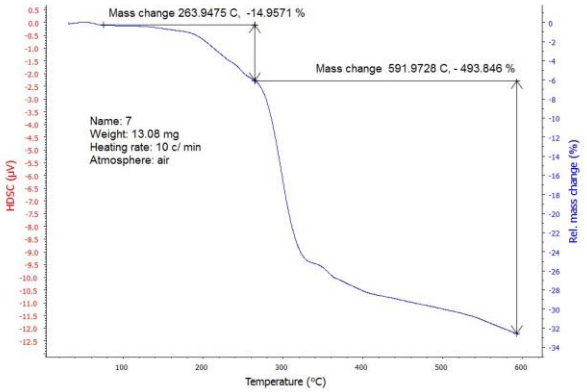

Figure (3-19) Thermal gravimetric of complex [$C_{20}H_{17}N_3O_6$Ni]

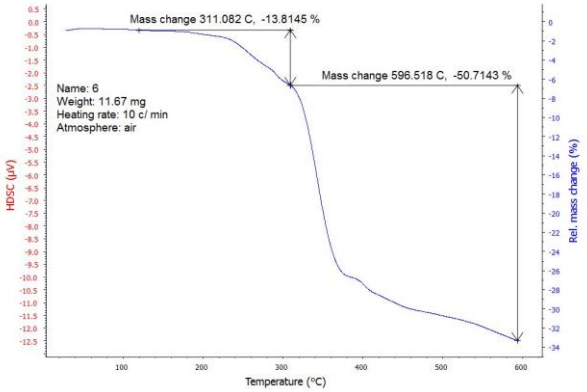

Figure (3-18) Thermal gravimetric of complex [$C_{21}H_{19}N_3O_6$ Ni]

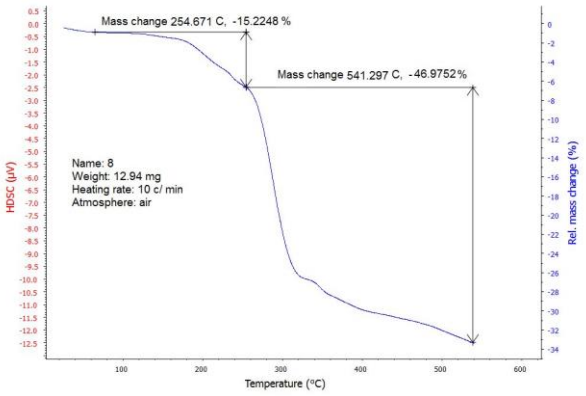

Figure (3-20) Thermal gravimetric of complex [$C_{18}H_{17}N_3O_9$ Ni Na_2P_2]

3-5 Equations for preparing ligands and nickel complexes

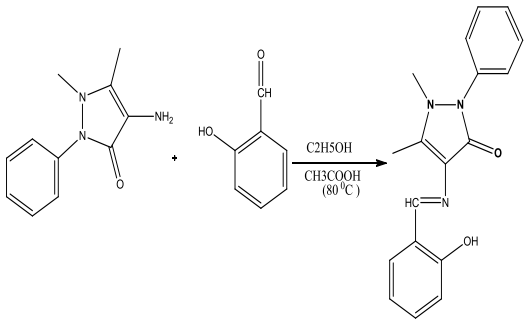

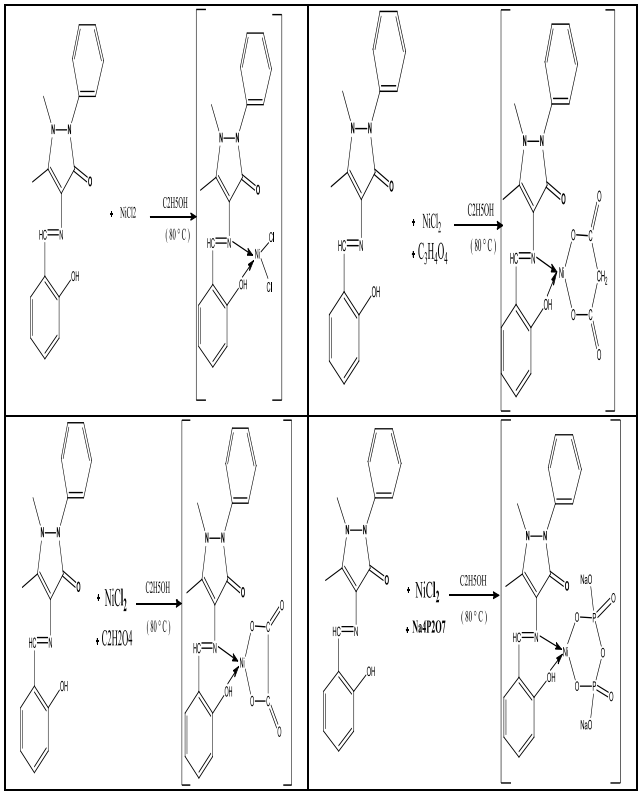

Effect of PH

An investigation was conducted to examine the influence of pH on the formation of the Ni (II) complex in an aqueous solution within a pH range of 2–11. To carry out this analysis, aliquots of 1.0 mL of a 10-3 ligand solution were transferred using a pipette to 1.0 mL of a 10-3 Ni (II) solution in volumetric flasks (10 mL). The flasks were then filled to a volume of 10.0 mL with a phosphate buffer solution with 2–11 pH. The solutions were measured for absorbance at a wavelength of 429 nm. The ligand's absorption spectra did not exhibit a complicated absorption peak, as shown in **Figure (3-21)**.

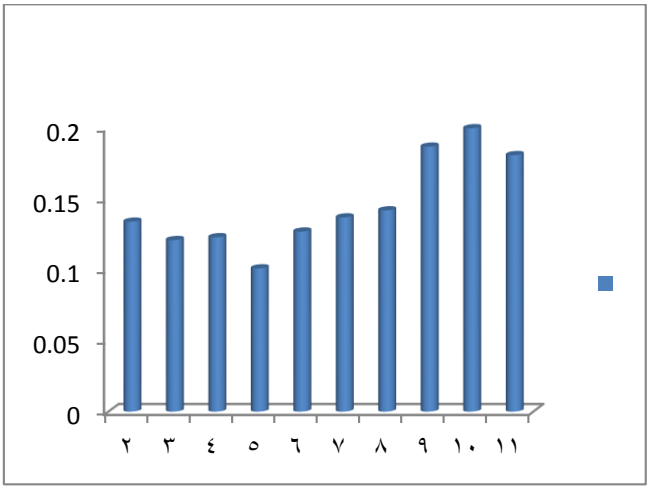

Figure (3-21) 3-7 Mole ratio method

The stoichiometry of complexes was determined using the mole ratio technique. This method involves measuring the absorbance of various solutions containing high concentrations of ligands and a stable concentration of metal ions at a specific maximum wavelength, where neither component absorbs light.[20] An association was found between molar absorbance, depicted on the y-axis, and the molar ratio of metal to ligand in the mixing solutions, depicted on the x-axis. Straight lines were drawn based on the linear regions of the data, and the detection point was identified, representing the stoichiometric ratio of metal to ligand in the resulting complex. The goal is to determine the molar ratio of each metal ion in its corresponding complex. Notably, the intensity of the complex's coloration increased progressively as the mixture approached this intersection point, indicating the optimal metal-to-ligand ratio. Beyond this point, the color intensity remained constant, indicating that the produced compound is stable under these conditions.[21]

Table (3-7) Absorption and concentration results for molar ratio

Ni (ml)	Ni (ppm)	L(ml)	L(ppm)	L/Ni (ppm)	Absorbance
1	5.8	0.25	7.675	1.32326	0.149
1	5.8	0.50	15.35	2.646552	0.215
1	5.8	0.75	23.025	3.969828	0.312
1	5.8	1	30.7	5.293103	0.364
1	5.8	1.25	38.375	6.616379	0.398
1	5.8	1.50	46.05	7.939655	0.411
1	5.8	1.75	53.725	9.262931	0.413
1	5.8	2	61.4	10.58621	0.42

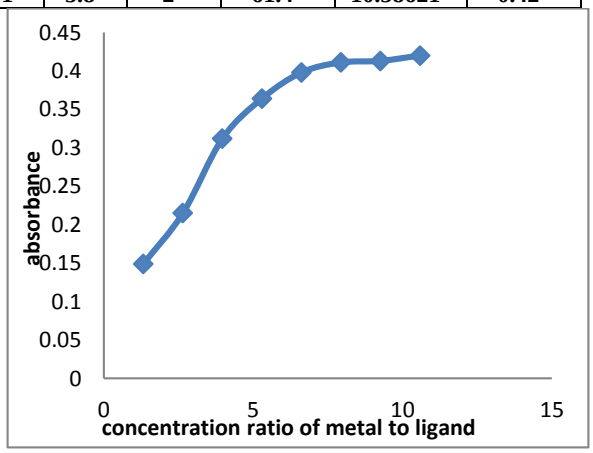

Figure 3-22 Curve mole ratio for determining the ratio of L to Ni.

Continuous change methods

A set of solutions were created with a pH of 11, and varying amounts of the ligand were combined while maintaining a consistent final volume. Curves were plotted, correlating the absorbance on the y-axis with the mole fraction on the x-axis. We derived the mole ratio (ligand to metal) by determining the junction of straight lines.[22]

Ni (ml)	L(ml)	Mole fraction	Absorbance
0	2	0	0.147
0.2	1.8	0.1	0.179
0.4	1.6	0.2	0.236
0.6	1.4	0.3	0.275
0.8	1.2	0.4	0.298
1	1	0.5	0.312
1.2	0.8	0.6	0.299
1.4	0.6	0.7	0.251
1.6	0.4	0.8	0.207

1.8	**0.2**	**0.9**	**0.139**
2	**0**	**1**	**0.101**

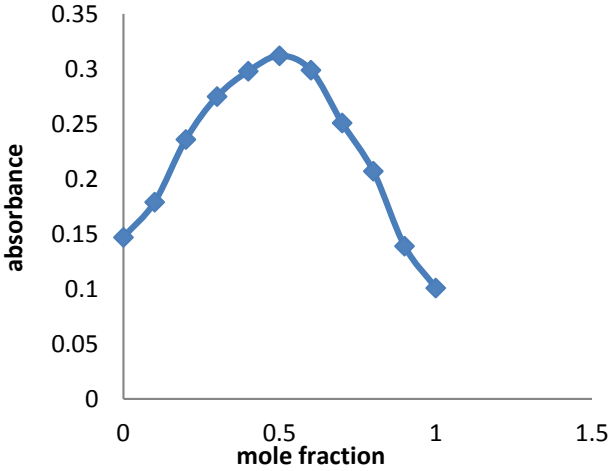

Figure 3-23 Curve of the Gob method to the Ni/L ratio

Conclusion

We prepared nickel complexes and examined their physical characteristics, performing numerous analytics. Using the Schiff base ligand (E)-4-((2-hydroxybenzylidene)amino)-1,5-dimethyl-2-phenyl-1,2-dihydro-3H-pyrazol-3-one and secondary ligands (malonic acid, oxalic acid, and pyrophosphate tetrasodium), information was collected. The results of electronic spectroscopy, infrared spectroscopy, mass spectrometry, and thermogravimetric analysis, and molar conduction and atomic absorption measurements indicated that all the Ni(II) complexes contained four coordinates. Molar conductivity measurements revealed a tetrahedral geometry. The structures all have the formula [Ni($C_{18}H_{17}N_3O_2$)(X)], where X is Cl2, malonic acid, oxalic acid, or pyrophosphate tetrasodium. Notably, ll the complexes were non-electrolytes. We can estimate palladium spectrophotometrically, using the reagent (E)-4-((2-hydroxybenzylidene)amino)-1,5-dimethyl-2-phenyl-1,2-dihydro-3H-pyrazol-3-one.

References

[1] ahmed Salem, H. Ali, and O. Al-Obaidi, "Preparation and Characterization of Fluorone Ligand Complexes for Co+2, Mn+2, and Fe+2 Metallic Ions," *Journal of University of Anbar for Pure Science*, vol. 17, no. 2, pp. 126–133, 2023, doi: 10.37652/juaps.2023.141636.1095.

[2] O. A. El-Gammal, F. S. Mohamed, G. N. Rezk, and A. A. El-Bindary, "Synthesis, characterization, catalytic, DNA binding and antibacterial activities of Co(II), Ni(II) and Cu(II) complexes with new Schiff base ligand," *Journal of Molecular Liquids*, vol. 326, p. 115223, 2021, doi: 10.1016/j.molliq.2020.115223.

[3] S. Menati, R. Azadbakht, H. A. Rudbari, and G. Bruno, "Synthesis and characterization of four new azo-Schiff base and their nickel(II) complexes," *Polyhedron*, vol. 205, p. 115296, 2021, doi: 10.1016/j.poly.2021.115296.

[4] N. P. Ebosie, M. O. C. Ogwuegbu, G. O. Onyedika, and F. C. Onwumere, *Biological and analytical applications of Schiff base metal complexes derived from salicylidene-4-aminoantipyrine and its derivatives: a review*, vol. 18, no. 12. Springer Berlin Heidelberg, 2021. doi: 10.1007/s13738-021-02265-1.

[5] A. M. Hassan, A. O. Said, B. H. Heakal, A. Younis, W. M. Aboulthana, and M. F. Mady, "Green Synthesis, Characterization, Antimicrobial and Anticancer Screening of New Metal Complexes Incorporating Schiff Base," *ACS Omega*, vol. 7, no. 36, pp. 32418–32431, 2022, doi: 10.1021/acsomega.2c03911.

[6] O. A. El-Gammal, A. A. El-Bindary, F. Sh. Mohamed, G. N. Rezk, and M. A. El-Bindary, "Synthesis, characterization, design, molecular docking, anti COVID-19 activity, DFT calculations of novel Schiff base with some transition metal complexes," *Journal of Molecular Liquids*, vol. 346, p. 117850, 2022, doi: 10.1016/j.molliq.2021.117850.

[7] H. A. K. Kyhoiesh and K. J. Al-Adilee, "Synthesis, spectral characterization, antimicrobial evaluation studies and cytotoxic activity of some transition metal complexes with tridentate (N,N,O) donor azo dye ligand," *Results in Chemistry*, vol. 3, p. 100245, 2021, doi: 10.1016/j.rechem.2021.100245.

[8] M. Yadav, S. Sharma, and J. Devi, "Designing, spectroscopic characterization, biological screening and antioxidant activity of mononuclear transition metal complexes of bidentate Schiff base hydrazones," *Journal of Chemical Sciences*, vol. 133, no. 1, 2021, doi: 10.1007/s12039-020-01854-6.

[9] Y. Li *et al.*, "Synthesis of Amino Acid Schiff Base Nickel (II) Complexes as Potential Anticancer Drugs in Vitro," *Bioinorganic Chemistry and Applications*,

vol. 2020, no. Ii, 2020, doi: 10.1155/2020/8834859.

[10] B. Shafaatian, A. Soleymanpour, N. Kholghi Oskouei, B. Notash, and S. A. Rezvani, "Synthesis, crystal structure, fluorescence and electrochemical studies of a new tridentate Schiff base ligand and its nickel(II) and palladium(II) complexes," *Spectrochimica Acta - Part A: Molecular and Biomolecular Spectroscopy*, vol. 128, pp. 363–369, 2014, doi: 10.1016/j.saa.2014.02.179.

[11] O. H. S. Al-Obaidi, "Binuclear Cu(II) and Co(II) complexes of tridentate heterocyclic shiff base derived from salicylaldehyde with 4-aminoantipyrine," *Bioinorganic Chemistry and Applications*, vol. 2012, pp. 1–7, 2012, doi: 10.1155/2012/601879.

[12] D. Aggoun *et al.*, "New nickel (II) and copper (II) bidentate Schiff base complexes, derived from dihalogenated salicylaldehyde and alkylamine: Synthesis, spectroscopic, thermogravimetry, crystallographic determination and electrochemical studies," *Polyhedron*, vol. 187, p. 114640, 2020, doi: 10.1016/j.poly.2020.114640.

[13] V. Adimule, B. C. Yallur, V. Kamat, and P. M. Krishna, "Characterization studies of novel series of cobalt (II), nickel (II) and copper (II) complexes: DNA binding and antibacterial activity," *Journal of Pharmaceutical Investigation*, vol. 51, no. 3, pp. 347–359, 2021, doi: 10.1007/s40005-021-00524-0.

[14] E. M. Zayed, G. G. Mohamed, and A. M. M. Hindy, "Transition metal complexes of novel Schiff base," 2014, doi: 10.1007/s10973-014-4061-3.

[15] S. H. Kadhim, I. Q. Abd-alla, and T. J. Hashim, "Synthesis and Characteristic Study of Co (II), Ni (II) and Cu (II) Complexes of New Schiff Base Derived from 4-Amino Antipyrine," *International Journal of Chemical Sciences*, vol. 15, no. 1, pp. 5–13, 2017.

[16] M. Q. Abdulridha and A. A. S. Al-Hamdani, "Synthesis, Characterization of New Metal Complexes of Co (II), Cu (II), Cd (II) and Ru (III) from azo ligand 5-((2-(1H-indol-2-yl)ethyl) diazinyl)-2aminophenol, Thermal and Antioxidant Studies," *Baghdad Science Journal*, vol. 20, pp. 1964–1975, 2023, doi: 10.21123/bsj.2023.7629.

[17] M. Q. Abdulridha, A. A. S. Al-Hamdani, and W. A. Mahmoud, "Synthesis, Characterization and Thermal Study of Some New Metal Ions Complexes with a New Azo 2-((2-(1H-Indol-2-yl)ethyl)diazinyl)-5-aminophenol," *Journal of Medicinal and Chemical Sciences*, vol. 6, no. 1, pp. 121–131, 2023, doi: 10.26655/JMCHEMSCI.2023.1.15.

[18] I. S. Hamza, W. A. Mahmmoud, A. A. Al-Hamdani, S. D. Ahmed, A. W. Allaf, and W. Al Zoubi, "Synthesis, characterization, and bioactivity of several metal complexes of (4-Amino-N-(5-methyl-isaxazol-3-yl)-benzenesulfonamide)," *Inorganic Chemistry Communications*, vol. 144, no. July, p. 109776, 2022, doi: 10.1016/j.inoche.2022.109776.

[19] M. J. Kareem, A. A. S. Al-Hamdani, Y. G. Ko, W. Al Zoubi, and S. G. Mohammed, "Synthesis, characterization, and determination antioxidant activities for new Schiff base complexes derived from 2-(1H-indol-3-yl)-ethylamine and metal ion complexes," *Journal of Molecular Structure*, vol. 1231, p. 129669, 2021, doi: 10.1016/j.molstruc.2020.129669.

[20] S. H. Jawad and K. J. Al-Adilee, "Synthesis and characterization of a new 1-methyl imidazole derived ligand with its ionic complexes Pd(II) and Pt(IV) and study of biological activity as anticancer and antioxidant," *Results in Chemistry*, vol. 4, no. October, p. 100573, 2022, doi: 10.1016/j.rechem.2022.100573.

[21] W. A. Ali, H. H. Mihsen, and S. H. Guzar, "Novel Derivative For Dithiocarbamite Containing A New Sulphur-Azo Linkage And Its Complexes With Sn(II), Sn(IV), Co(II), Ni(II) And Cu(II) Ions; Synthesis, Characterization and Antibacterial Activity," *Al-Bahir Journal for Engineering and Pure Sciences*, vol. 2, no. 1, 2023, doi: 10.55810/2313-0083.1016.

[22] A. M. Abu-Dief *et al.*, "Synthesis and characterization of new Cr(III), Fe(III) and Cu(II) complexes incorporating multi-substituted aryl imidazole ligand: Structural, DFT, DNA binding, and biological implications," *Spectrochimica Acta - Part A: Molecular and Biomolecular Spectroscopy*, vol. 228, no. Iii, p. 117700, 2020, doi:

P- ISSN 1991-8941 E-ISSN 2706-6703 *Journal of University of Anbar for Pure Science (JUAPS)* Open Access
2025,(19), (01):137 – 149

10.1016/j.saa.2019.117700.

تحضير، تشخيص ودراسة حرارية لمعقدات النيكل الثنائي مع قواعد شيف وليكاندات مختلطه وتطبيقاتها التحليلية

وصال صادق احميد ، ستار رجب مجيد

قسم الكيمياء ،كلية العلوم ، جامعة الأنبار ، الأنبار ، العراق
wis22s3001@uoanbar.edu.iq , sat70tar@uoanbar.edu.iq

الخلاصة:

تم تحضير معقدات النيكل من قاعدة شيف (**C18H17N302**) كمادة أولية ، وحمض الأكساليك وحمض المالونيك وبيروفوسفات الصوديوم كمركبات ثانوية بنسبة مولية (1 : 1). تم تشخيص المعقدات بواسطة التحليل المجهري للعناصر، الامتصاص الذري التحليل الطيفي الكتلي، التحليل الوزني الحراري، التحليل الطيفي **FT–IR**، التحليل الطيفي فوق البنفسجي، التوصيلية المولارية، ودرجة الانصهار. كان للمعقدات الناتجة شكل مربع مستوي تم قياسها كميًا عند الطول الموجي الاقصى 429 نانومتر. أشارت النتائج إلى أن جميع المعقدات غير إلكتروليتية وروابط قاعدة شيف (**C18H17N302**)، حمض الأكساليك والمالونيك، وبيروفوسفات الصوديوم يتصرفان كروابط ثنائية المسننة مع أيونات النيكل (**II**). واستنادا الى النتائج السابقه فأن كاشف (**C18H17N302**) يمكن استخدامه في تقدير أيونات النيكل في المحاليل الملونه حسب قانون لامبرت بير .